8

Traffic Conformance Study

In this chapter, we will apply stochastic network calculus to a traffic conformance study.

To achieve a certain level of quality of service (QoS) assurance, a network will have service level agreements (SLAs) with its users and neighboring domains, which, in general, describe the QoS level that the service provider is committed to provide and the specification of traffic that users or neighboring domains are allowed to send for the subscribed QoS level. For example, in a Differentiated Services network [10], all incoming flows must conform to a certain pre-determined SLA and the conformance is measured by a policer at the ingress router of the network. Based on the SLA, the network will provide a certain level of QoS to the conformant part of these flows. Since flows may interact with each other and compete for resources at each node of a network, an interesting and important question arises as to whether a flow is still conformant to its original traffic specification after crossing the network.

This chapter considers conformance deterioration for both individual flows and aggregates of flows. In some situations, an individual flow needs to negotiate SLAs with networks along its end-to-end path. In this case, the per-flow conformance deterioration along its end-to-end path is considered. Another case is also considered where the individual user only needs to establish an SLA with the first access network, and the access network will negotiate a bulk SLA with its next intermediate network for the corresponding aggregate of flows. For example, several users may subscribe to the same level of service, each has its individual SLA with the first access network, and traffic from these users is aggregated in the same class. When such an aggregate exits the first network and enters the next network, the aggregate will be checked for its conformance based on the bulk SLA between these two domains.

In this chapter, we study analytically the extent to which a flow and an aggregate of flows become non-conformant in two typical network scenarios. In particular, we investigate conformance deterioration in a per-flow scheduling network where network servers guarantee a certain level of service to each flow and in an aggregate scheduling network where network servers provide a

Y. Jiang, Y. Liu, *Stochastic Network Calculus*,
DOI: 10.1007/978-1-84800-127-5_8,

certain level of service to each aggregation of flows to support scalable QoS provisioning. Based on a relationship between the conformance deterioration and stochastic burstiness increase that will be established in this chapter and results from the previous chapters, analytical bounds on conformance deterioration probability are presented for both the per-flow and the per-aggregate cases.

8.1 Network Model

Consider a network as shown in Figure 8.1. In this network, every incoming flow under consideration is shaped by a token bucket shaper at an ingress router, whose token generation rate and bucket size are set based on some pre-determined SLA. At the corresponding egress router a token bucket meter with the same parameters as the ingress shaper checks the conformance of its outgoing traffic. If the burstiness of the input flow increases and consequently some packets of the flow do not conform to the token bucket meter at the egress, they will be marked as OUT of profile. This chapter is concerned with the conformance deterioration probability, which is defined as the ratio of the number of OUT packets to that of received packets recorded in the token bucket meter at the egress router. The two network scenarios under investigation are per-flow scheduling networks, where network servers guarantee a certain level of service to each flow, and aggregate scheduling networks, where network servers provide a certain level of service to each aggregation of flows.

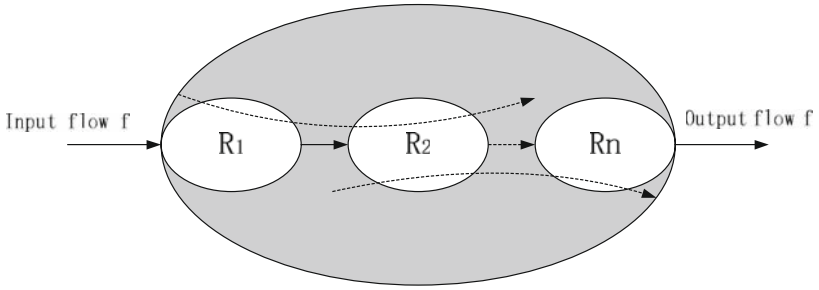

Fig. 8.1. Network model

The burstiness increase for a flow after crossing a certain network element was first studied by Cruz [28][29] in a deterministic framework. Reference [28] obtained the burstiness of an output flow given the burstiness of the input flow. Some recent works [92][22] studied the worst-case burstiness increase under aggregate scheduling. However, these deterministic bounds on worst-case burstiness increase cannot be used to obtain the conformance deterioration probability since the conformance deterioration probability is a stochastic

metric. Hence, the stochastic burstiness increase needs to be investigated in order to determine the conformance deterioration probability. To study the stochastic burstiness increase of an input flow after crossing a network, the initial stochastic characterization of the flow before being shaped by the token bucket is needed. The m.b.c stochastic arrival curve concept described in previous chapters is used to model an input traffic process before it enters the network. Here, it is assumed that the bounding functions for all input flows of interest are known or can be easily obtained. The deterministic service curve, stochastic service curve, and stochastic strict service curve concepts as explained in previous chapters are used to model servers in this chapter.

8.1.1 Conformance Deterioration and Stochastic Burstiness Increase

To analytically calculate the bound of the conformance deterioration probability for a flow checked by a token bucket meter, the same flow is fed to a virtual server with a constant service rate that is the same as the token generation rate of the token bucket meter. This section will establish the relationship between conformance deterioration probability and stochastic burstiness increase measured in the virtual server fed with the same input flow. The following theorem shows that the probability that a packet is marked as OUT by the token bucket meter is bounded by the probability that the queue length in the virtual server exceeds the bucket depth of the token bucket meter.

Theorem 8.1 (Relationship between Non-conformance and Stochastic Burstiness). *Consider a flow fed into a token bucket meter and a virtual initially empty constant-rate server, respectively. The token bucket has parameters* (ρ, σ_{th})*, where* ρ *is the token generation rate and* σ_{th} *is the bucket depth. The constant-rate server has service rate* ρ*. Then,* $P_{nonconf}(t) \leq P_{W(t;r)>\sigma_{th}} \leq P_{M(t;r)>\sigma_{th}}$ *where* $P_{nonconf}(t)$ *denotes the probability that one packet is found to be OUT,* $W(t;r) \equiv \sup_{0\leq s\leq t}\{A(s,t) - r(t-s)\}$*, which is the queue length at the constant-rate server,* $P_{W(t;r)>\sigma_{th}}$ *is the probability that the queue length* $W(t;r)$ *in the constant rate server exceeds* σ_{th}*,* $M(t;r) \equiv \sup_{0\leq s\leq t} \sup_{0\leq u\leq s}[A(u,s) - r(s-u)]$*, which is the maximum up-to-date backlog at time* t *for the constant-rate server, and* $P_{M(t;r)>\sigma_{th}}$ *is the probability that the maximum up-to-date backlog* $M(t)$ *exceeds* σ_{th}*.*

Proof. Consider the case where one packet arriving at time t has been found non-conformant by the token bucket. Then, there exists some $s < t$ for which the amount of traffic arrival during $[s,t)$ satisfies:

$$A(s,t) > \rho(t-s) + \sigma_{th}.$$

Therefore,

$$\begin{aligned} P_{nonconf}(t) &\le P\{A(s,t) > \rho(t-s) + \sigma_{th}\} \\ &= P\{A(s,t) - \rho(t-s) > \sigma_{th}\} \\ &\le P\left\{\sup_{0\le s^*\le t}\{A(s^*,t) - \rho(t-s^*)\} > \sigma_{th}\right\} \\ &= P_{W(t;r)>\sigma_{th}} \\ &\le P\left\{\sup_{0\le s\le t}\sup_{0\le s^*\le s}\{A(s^*,s) - \rho(s-s^*)\} > \sigma_{th}\right\} \\ &= P_{M(t;r)>\sigma_{th}}. \end{aligned}$$

This completes the proof. □

With Theorem 8.1, it is clear that to obtain the bound for the conformance deterioration probability, one approach is to derive the queue length distribution of the output flow in the corresponding virtual server. Since the queue length distribution in the virtual server is characterized by a bounding function in the m.b.c. stochastic arrival curve definition, the bounding function is used here to characterize the stochastic burstiness for the flow of interested. Therefore, the bounding function of the output flow at the egress of a network is needed given the initial bounding function of the input flow at the ingress.

8.1.2 Property of Token Bucket Shaper

Since the token bucket shaper is the first network element passed by an incoming flow to the network, the following theorems provide insights into the output burstiness of the token bucket shaper, which will be used for subsequent analysis of conformance deterioration analysis.

Theorem 8.2 (Property of Token Bucket Shaper). *Consider a shaping system with token bucket shaper (ρ, σ). Let $A(t)$ and $A^*(t)$ be the input process and output process of the system, respectively. Assume that $A(t) \sim_{mb} \langle f, \rho\rangle$. Then, for any $t \ge 0$,*

$$A^*(t) \sim_{mb} \langle g, \rho\rangle, \tag{8.1}$$

where

$$g(x) = \begin{cases} f(x) & \text{if } x \le \sigma, \\ 0 & \text{if } x > \sigma. \end{cases} \tag{8.2}$$

Proof. Using a method similar to the proof of Theorem 5 in [140],

$$M^*(t;\rho) \le M(t;\rho),$$

where $M(t;\rho)$ and $M^*(t;\rho)$ denote the maximum up-to-date queue length in the virtual constant server for the input process and output process, respectively. In addition, the output traffic is constrained by the token bucket regulator; i.e., $A^*(s,t) \le \rho(t-s) + \sigma$. Hence,

$$M^*(t;\rho) = \sup_{0\le s\le t}\sup_{0\le u\le s}\{A^*(s,u) - \rho(u-s)\} \le \sigma,$$

which implies that, for any $x > \sigma$, $P\{M^*(t;\rho) \ge x\} = 0$. This, together with the above, ends the proof. □

8.2 Conformance Study of Per-Flow Scheduling Network

This section studies conformance deterioration of a flow after crossing a per-flow scheduling network. To study the end-to-end conformance deterioration, the single-node case is considered first and then the results are extended to the multi-node case.

8.2.1 Single-Node Case

Theorem 5.21 in Chapter 5 derived the stochastic burstiness of the output flow after crossing a node that offers a stochastic service curve to the input flow with an m.b.c. stochastic arrival curve. Then, based on the relationship between stochastic burstiness and non-conformance derived in Theorem 8.1, one can immediately obtain the following theorem on the non-conformance probability of a flow after crossing a node that offers a service curve to the input flow.

Theorem 8.3 (Single-Node Non-conformance Probability Bound). *Assume that a node offers a deterministic service curve β to its input. Let $A(t)$ be the input process of the node. Assume that $A(t) \sim_{mb} \langle f, r\rangle$. The output flow is checked for its conformance by a token bucket meter with token generation rate r and token bucket depth σ_{th}. Let $P_{nonconf}(t)$ denote the probability that one packet is found to be OUT. Thus,*

$$P_{nonconf}(t) \le f(\sigma_{th} - \alpha \oslash \beta(0)), \tag{8.3}$$

where $\alpha(t) = rt$ and $\alpha \oslash \beta(0) = \sup_{s\ge 0}\{\alpha(s) - \beta(s)\}$.

Reference [53] presents another general server model, which is the guaranteed rate (GR) server model. It has been proven that many well-known schedulers belong to GR (e.g., see [68] and references therein), as mentioned earlier in Chapter 2. The behavior of a GR server is determined by two parameters: a rate R and an error term E. In [92], it was proven that a GR node has a rate-latency service curve $\beta(t)$: $\beta(t) = R(t - E - \frac{L_{\max,i}}{R})^+$, where $L_{\max,i}$ is the maximum packet size of the input flow. Therefore, the following corollary can be derived directly by using the service curve of a GR scheduler to analyze the stochastic burstiness increase of a flow after it passes through the GR scheduler.

Corollary 8.4 (Non-conformance Probability Bound under a GR Node). *Consider a GR node with rate R and error term E. Let $A(t)$ be the input process of the node. Assume that $A(t) \sim_{mb} \langle f, \rho \rangle$. The output flow is checked for its conformance by a token bucket meter with token generation rate ρ and token bucket depth σ_{th}. Let $P_{nonconf}(t)$ denote the probability that one packet is found to be OUT. Given $\rho \leq R$, for any $t > 0$,*

$$P_{nonconf}(t) \leq f\left(\sigma_{th} - \rho\left(E + \frac{L_{\max,i}}{R}\right)\right), \tag{8.4}$$

where $L_{\max,i}$ is the maximum packet size of the flow under consideration.

Remark. For a WFQ scheduler, the error term is $E = \frac{L\max}{C}$, where C is its total capacity and the $L_{\max}$ is the maximum packet size among all flows in the same server. Hence, it has a rate-latency service curve $\beta(t) = R\left(t - E - \frac{L\max,i}{R}\right)^+$. According to the corollary above under WFQ, the output traffic burstiness bounding function for an input flow with bounding function $f(x)$ will be $g(x) = f(x - \alpha \oslash \beta(0)) = f\left(x - \rho\left(\frac{L_{\max}}{C} + \frac{L_{\max,i}}{R}\right)\right)$. From this bounding function, it can be seen that, even for a WFQ scheduler that can provide service isolation among different service classes, if the packet size $L_{\max}$ of inter-class traffic is large enough compared with the packet size $L_{\max,i}$ of the flow under consideration, the effect of inter-class traffic on conformance deterioration of the flow considered cannot be ignored.

8.2.2 Multi-node Case

This section studies the conformance deterioration of a flow crossing a network of nodes in tandem. Suppose that there are a total of N nodes and each node i provides a service curve β_i to the flow. Then, according to the concatenation property of a deterministic service curve as shown in Chapter 2, the network provides to the flow a concatenated deterministic service curve to the flow that is given by

$$\beta_{net} = \beta_1 \otimes \beta_2 \cdots \otimes \beta_N. \tag{8.5}$$

With this concatenated deterministic service curve and Theorem 8.1, the following result is immediately obtained.

Theorem 8.5 (Multi-node Non-conformance Probability Bound). *Consider a flow crossing a path with N nodes in tandem, and each node i provides deterministic service curve β_i to the flow. Let $A(t)$ be the input process of the flow and $A(t) \sim_{mb} \langle f, r \rangle$. The output flow is checked for its conformance by a token bucket meter with token generation rate r and token bucket depth σ_{th}. Then, the non-conformance probability $P_{nonconf}(t)$ at the egress is bounded by*

$$P_{nonconf}(t) \leq f(\sigma_{th} - \alpha \oslash \beta_{net}(0)), \tag{8.6}$$

where $\alpha(t) = rt$ and $\beta_{net} = \beta_1 \otimes \beta_2 \cdots \otimes \beta_N$.

By using Theorem 8.2, the m.b.c. bounding function can be obtained for the input traffic after passing through the token bucket shaper at the ingress of the network. Then, the end-to-end non-conformance probability of the output flow at the egress of the network can be further obtained by applying Theorem 8.5.

8.3 Conformance Study of Aggregate Scheduling Network

To provide scalable support of QoS in a network, one method is to let each node in the network provide service to aggregates of flows. By doing this, the core node does not need to maintain per-flow state information. In such a network, each node performs aggregate scheduling instead of per-flow scheduling. This section first conducts conformance analysis for each flow within the aggregate under aggregate scheduling and then analyzes conformance deterioration for each aggregate.

8.3.1 Per-Flow in Single-Node Case

Following the same approach as in Section 8.2, this section studies the conformance deterioration by analyzing the stochastic burstiness increase of input flows, for which the per-flow service received by a flow within the aggregate is required. From Theorem 2.27 in Chapter 2, we have the following results. For a node serving two flows f and h, if the node guarantees a deterministic service curve β to the aggregate of the two flows and flow h has an arrival curve α^h, then the node offers to the flow f a deterministic service curve $\beta^f = \left(\beta - \alpha^h\right)^+$.

Based on this per-flow service curve, one can obtain a result on the per-flow stochastic burstiness increase under aggregate scheduling by applying this leftover deterministic service curve to results in Chapter 5. Note that the per-flow service curve used in this approach is a deterministic service curve that is derived under the assumption that all the input flows are deterministically bounded. In addition, the resulting bound on conformance deterioration is the worst-case bound. Since the traffic model used in this chapter is a stochastically bounded traffic model, it would be possible to get a more accurate characterization of the per-flow service in a stochastic form, which enables tighter bounds to be obtained in conformance analysis.

Theorem 8.6 (Per-Flow Stochastic Burstiness Bound under Deterministic Per-Flow Service Curve). *Consider a node providing a deterministic service curve β to two flows f and h, that are FIFO-aggregated. Let $A_i(t)$ and $A_i^*(t)$ be the flow i $(i = f, h)$ input process and output process of the node, respectively. Suppose that $A_f(t) \sim_{mb} \langle f^f, r^f \rangle$ and $A_h(t)$ is token bucket bounded by (r^h, σ^h). Then,*

$$A_f^*(t) \sim_{mb} \left\langle \left[g^f\right]_1, r^f \right\rangle \tag{8.7}$$

with

$$g^f(x) = f^f\left(x - \alpha^f \oslash \beta^f(0)\right), \tag{8.8}$$

where $\alpha^f(t) = r^f t$, $\beta^f = \left(\beta - \alpha^h\right)^+$.

Remark. Based on Theorem 8.6 on the per-flow stochastic burstiness and Theorem 8.1, the following result on the non-conformance probability bound is immediately obtained.

Theorem 8.7 (Per-Flow Non-conformance Bound under Deterministic Per-Flow Service Curve). *Consider a node providing a deterministic service curve* β *to two flows* f *and* h *that are FIFO-aggregated. Let* $A_i(t)$ *be the flow* i $(i = f, h)$ *input process of the node. Suppose that* $A_f(t) \sim_{mb} \left\langle f^f, r^f \right\rangle$ *and* $A_h(t)$ *is token bucket bounded by* (r^h, σ^h)*. The output flow is checked for its conformance by a token bucket meter with token generation rate* r^f *and token bucket depth* σ_{th}*. Let* $P_{nonconf}(t)$ *denote the probability that one packet is found to be OUT. Then,*

$$P_{nonconf}(t) = f^f\left(\sigma_{th} - \alpha^f \oslash \beta^f(0)\right), \tag{8.9}$$

where $\alpha^f(t) = r^f t$, $\beta^f = \left(\beta - \alpha^h\right)^+$.

Remark. The service curve used in this theorem is the worst-case leftover deterministic service curve within an aggregate under aggregate scheduling. However, if the cross traffic aggregated in the same aggregate is stochastically bounded, one can have a tighter and more accurate characterization of the per-flow service received by a flow under aggregate scheduling, which is derived in Chapters 5 and 6. For this, we need to derive the stochastic leftover service curve, then derive the burstiness increase for the input processes, and then derive the non-conformance probabilities for these input processes after passing a server under aggregate scheduling.

Lemma 8.8 (Stochastic Per-Flow Service Curve under Aggregate Scheduling for General Case). *Consider a server fed with a flow* A *that is the aggregation of two constituent flows* A_f *and* A_h*. Suppose the server provides a deterministic service curve* β *to the aggregate flow* A*. If flow* A_h *has an m.b.c. stochastic arrival curve* $A_h \sim_{mb} \langle f^h, r^h \rangle$ *and* $\beta^f \in \mathcal{F}$*, then the server guarantees to flow* A_f *a stochastic service curve* $S_f \sim_{sc} \langle f^h, \beta^f \rangle$*, where*

$$\beta^f(t) = \beta(t) - r^h(t), \tag{8.10}$$

$$g^f(x) = f^h(x). \tag{8.11}$$

Proof. Theorem 5.42 in Chapter 5 obtained the following result on the per-flow stochastic service for a system with a stochastic service curve and m.b.c.

stochastic arrival curve. Then, flow f receives a per-flow stochastic service curve $\left(f^f, \beta^f\right)$ from the node with

$$\beta^f(t) = \beta(t) - r^h(t),$$
$$f^f(x) = f^h \otimes 0(x) = f^h(x).$$

□

Lemma 8.8 shows that a deterministic server under aggregate scheduling can be considered a stochastic service providing a per-flow stochastic service curve to its input flows. Based on this per-flow stochastic service curve, we can derive the burstiness increase for these input processes.

Theorem 8.9 (Per-Flow Stochastic Burstiness Bound under Stochastic Per-Flow Service Curve for General Case). *Consider a node providing a deterministic service curve β to two flows f and h that are FIFO-aggregated. Let $A_i(t)$ and $A_i^*(t)$ be the flow i $(i = f, h)$ input process and output process of the node, respectively. Suppose that $A_h(t) \sim_{mb} \left\langle f^h, r^h \right\rangle$ and $A_f(t) \sim_{mb} \left\langle f^f, r^f \right\rangle$. Then, we have $A_f^*(t) \sim_{mb} \left\langle f^{f*}, r^{f*} \right\rangle$ with*

$$f^{f*}(x) = f^f \otimes f^h(x), \tag{8.12}$$
$$r^{f*}(t) = r^f(t) \oslash \left(\beta(t) - r^h(t)\right). \tag{8.13}$$

Proof. Based on the per-flow stochastic service derived in Lemma 8.8, the stochastic burstiness increase of a flow under aggregate scheduling can be derived according to Theorem 5.21 in Chapter 5. In this case, for any $t \geq 0$,

$$A_f^*(t) \sim_{mb} \left\langle f^{f*}, r^{f*} \right\rangle$$

with

$$r^{f*}(t) = r^f(t) \oslash \left(\beta(t) - r^h(t)\right),$$
$$f^{f*}(x) = f^f \otimes f^h(x).$$

□

Note that the result above is derived under the case where it is not known whether the two input processes are independent or not. If the server can be modeled by a stochastic strict service curve and the service process is independent of the two independent input processes, we can have the following tighter results for the per-flow stochastic burstiness bound.

Lemma 8.10 (Stochastic Leftover Service Curve under Aggregate Scheduling for Independent Case). *Consider a server fed with a flow A that is the aggregation of two constituent independent flows A_f and A_h. Suppose the server provides a deterministic strict service curve β to the aggregate flow A. If flow A_h has the m.b.c. stochastic arrival curve $A_h \sim_{mb} \langle f^h, r^h \rangle$ and*

$\beta^f \in \mathcal{F}$, then flow f receives a stochastic strict service curve β with impairment process $I = A_h(t) - A_h(t-s)$. *Then, the server guarantees to flow A_f stochastic service curve $S_f \sim_{sc} \langle f^h, \beta^f \rangle$, where*

$$\beta^f(t) = \beta(t) - r^h(t), \tag{8.14}$$

$$g^f(x) = f^h(x). \tag{8.15}$$

Proof. According to the definition of a deterministic strict service curve, during any backlogged period $[s,t)$, we can have, for all $t \geq 0, A^*(t) \geq A(t-s) + \beta(s)$. Then

$$A_f^*(t) + A_h^*(t) \geq \beta(s) + A_f(t-s) + A_h(t-s).$$

Since $A_h^*(t) \leq A_h(t)$,

$$A_f^*(t) - A_f(t-s) \geq \beta(s) - (A_h(t) - A_h(t-s)).$$

Since $A_f^*(t-s) \leq A_f(t-s)$, we have

$$A_f^*(t) - A_f^*(t-s) \geq \beta(s) - (A_h(t) - A_h(t-s)).$$

Then, according to the definition of a stochastic strict service curve in Definition 4.11 in Chapter 4, flow f receives a *stochastic strict service curve* β with *impairment process* $I = A_h(t) - A_h(t-s)$.

In addition, we have $A_h(t) \sim_{mb} \left\langle f^h, r^h \right\rangle$. According to Lemma 8.8, the server provides a stochastic service curve $S^f \sim_{sc} \langle f^h, \beta^f \rangle$ for flow f with

$$\beta^f(t) = \beta(t) - r^h(t).$$

□

Theorem 8.11 (Per-Flow Stochastic Burstiness Bound under Stochastic Per-Flow Service Curve for Independent Case). *Consider a node providing a deterministic strict service curve β to two independent flows f and h that are FIFO-aggregated. Let $A_i(t)$ and $A_i^*(t)$ be the flow i $(i = f, h)$ input process and output process of the node, respectively. Suppose that $A_h(t) \sim_{mb} \left\langle f^h, r^h \right\rangle$ and $A_f(t) \sim_{mb} \left\langle f^f, r^f \right\rangle$. Then, we have $A_f^*(t) \sim_{mb} \left\langle f^{f*}, r^{f*} \right\rangle$ with*

$$r^{f*}(t) = r^f(t) \oslash \left(\beta(t) - r^h(t)\right), \tag{8.16}$$

$$f^{f*}(x) = 1 - \bar{f}^f * \bar{f}^h(x), \tag{8.17}$$

where $\bar{f}^f(x) = 1 - [f^f(x)]_1$ and $\bar{f}^h(x) = 1 - [f^h(x)]_1$.

Proof. Based on the leftover stochastic service curve obtained in Lemma 8.10, the stochastic burstiness increase of a flow under aggregate scheduling can be derived according to Theorem 6.5 in Chapter 6. In this case, for any $t \geq 0$,

$$A_f^*(t) \sim_{mb} \left\langle f^{f*}, r^{f*} \right\rangle$$

with

$$r^{f*}(t) = r^f(t) \oslash \left(\beta(t) - r^h(t)\right),$$
$$f^{f*}(x) = 1 - \bar{f}^f * \bar{f}^h(x),$$

where $\bar{f}^f(x) = 1 - [f^f(x)]_1$ and $\bar{f}^h(x) = 1 - [f^h(x)]_1$. □

With Theorem 8.1, the following results on non-conformance probability bound follow from Theorems 8.9 and 8.11.

Theorem 8.12 (Per-Flow Non-conformance Probability Bound under Aggregation for General Case). *Consider a node providing a service curve β to two flows f and h that are FIFO-aggregated. Let $A(t)$ be the input process of the node. Suppose that $A_h(t) \sim_{mb} \langle f^h, r^h \rangle$ and $A_f(t) \sim_{mb} \langle f^f, r^f \rangle$. The output of flow f is checked for its conformance by a token bucket meter with token generation rate r^f and token bucket depth σ_{th}. Let $P_{nonconf}(t)$ denote the probability that one packet is found to be OUT. Then*

$$P_{nonconf}(t) \leq f^f \otimes f^h\left(\sigma_{th} - \alpha^f \oslash \beta^f(0)\right), \tag{8.18}$$

where $\alpha^f(s) = r^f s$, $\alpha^f \oslash \beta^f(0) = \sup_{s \geq 0}\{\alpha^f(s) - \beta^f(s)\}$, and $\beta^f(s) = \beta(s) - r^h s$.

Theorem 8.13 (Per-Flow Non-conformance Probability Bound under Aggregation for Independent Case). *Consider a node providing a service curve β to two flows f and h that are FIFO-aggregated. Let $A(t)$ be the input process of the node. Suppose that $A_h(t) \sim_{mb} \langle f^h, r^h \rangle$ and $A_f(t) \sim_{mb} \langle f^f, r^f \rangle$. The output of flow f is checked for its conformance by a token bucket meter with token generation rate r^f and token bucket depth σ_{th}. Let $P_{nonconf}(t)$ denote the probability that one packet is found to be OUT. If the flows f and h are independent of each other, then*

$$P_{nonconf}(t) \leq 1 - \bar{f}^f * \bar{f}^h\left(\sigma_{th} - \alpha^f \oslash \beta^f(0)\right), \tag{8.19}$$

where $\alpha^f(t) = r^f t$, $\alpha^f \oslash \beta^f(0) = \sup_{s \geq 0}\{\alpha^f(s) - \beta^f(s)\}$, $\beta^f(s) = \beta(s) - r^h s$, $\bar{f}^f(\sigma) = 1 - \left[f^f(\sigma)\right]_1$, and $\bar{f}^h(\sigma) = 1 - \left[f^h(\sigma)\right]_1$.

Remark. When the per-flow non-conformance probability in the first server is analyzed, Theorem 8.13 can be used since the two flows are independent of each other. However, when they exit the first server, the result derived for the general case in Theorem 8.12 needs to be used to analyze the non-conformance probability in subsequent servers since they will no longer be independent of one another when they exit the server.

8.3.2 Per-Flow in Multi-node Case

As shown earlier, a series of stochastic service curves and stochastic strict service curves in tandem can be concatenated as a network stochastic service curve. Combining these results with the results derived above on the non-conformance probability bounds for the single-node case, we can have the following results on multi-node non-conformance probability bounds for the general case and independent case, respectively.

Theorem 8.14 (Multi-node Non-conformance Probability Bound for General Case). *Consider a flow f crossing a path with N nodes in tandem, and each node i provides a service curve β^i to the flows f and h_i, which are FIFO-aggregated. Suppose that $A_{h_i}(t) \sim_{mb} \left\langle f^{h_i}, r^{h_i} \right\rangle$ and $A_f(t) \sim_{mb} \left\langle f^f, r^f \right\rangle$. The output flow from the system is checked for its conformance by a token bucket meter with token generation rate r and token bucket depth σ_{th}. Then, the non-conformance probability $P_{nonconf}(t)$ is bounded by*

$$\begin{aligned} &P_{nonconf}(t) \\ &\leq f^f \otimes f^{h_1} \otimes \cdots \otimes f^{h_N} \left(\sigma - \alpha^f \oslash \left(\beta^{f_1} \otimes \cdots \otimes \beta^{f_N}\right)(0)\right), \end{aligned} \tag{8.20}$$

where $\alpha^f(t) \equiv r^f t$, and $\beta^{f_i}(t) = \beta^i(t) - r^{h_i}(t)$, $i = 1, \cdots, N$.

For a special case where all cross flows along the end-to-end path is independent with the flow of interested, a tighter bound can be obtained in the same way as Theorem 8.13.

Theorem 8.15 (Multi-Node Non-Conformance Probability Bound for Independent Case). *Consider a flow f crossing a path with N nodes in tandem and the i-th node providing a service curve β^i to two flows f and h_i that are FIFO-aggregated. Suppose that $A_{h_i}(t) \sim_{mb} \left\langle f^{h_i}, r^{h_i} \right\rangle$ and $A_f(t) \sim_{mb} \left\langle f^f, r^f \right\rangle$. The output flow f from the system is checked for its conformance by a token bucket meter with token generation rate r and token bucket depth σ_{th}. Then the non-conformance probability $P_{nonconf}(t)$ of flow f is bounded by*

$$P_{nonconf}(t) \leq 1 - \bar{f}^f * \bar{f}^{h_1} * \cdots * \bar{f}^{h_N} \left(\sigma - \alpha^f \oslash \left(\beta^{f_1} \otimes \cdots \otimes \beta^{f_N}\right)(0)\right), \tag{8.21}$$

where $\bar{f}^f(t) = 1 - \left[f^f(t)\right]_1$, $\bar{f}^{h_i} = 1 - \left[f^{h_i}\right]_1$, $\alpha^f(t) \equiv r^f t$, and $\beta^{f_i}(t) = \beta^i(t) - r^{h_i}(t)$, $i = 1, \cdots, N$.

The results presented in this section provide an approach for analyzing conformance deterioration of a flow after crossing an aggregate scheduling network. In particular, as illustrated in Figure 8.2, the procedures are as follows.

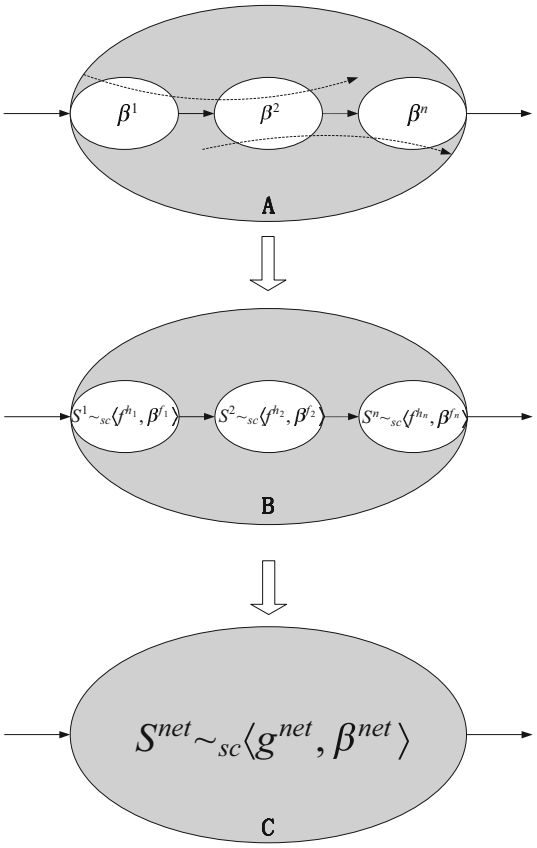

Fig. 8.2. Aggregate scheduling in multi-node case

Procedures to obtain the end-to-end non-conformance probability bound:

1. Determine the initial bounding functions f^f for the stochastic burstiness of flow f under consideration with rate r^f and each cross-flow in the same aggregate at each hop along the end-to-end path with rate r^{h_i}.

2. Determine the bounding functions for the stochastic burstiness of flow f after passing through a token bucket shaper according to Theorem 8.2.

3. Convert each aggregate scheduling server (providing a service curve to the aggregate) to a per-flow scheduling server (providing a stochastic service curve to the flow) according to Theorems 8.8 or 8.10 for general case or independent case, respectively.

4. Obtain the end-to-end non-conformance probability bound according to Theorems 8.14 or 8.15 for the general case or independent case, respectively.

8.3.3 Per-Aggregate Case

All the results above can be used to analyze the conformance deterioration of an individual flow when it negotiates SLAs with networks along its end-to-end path. However, there is another service configuration mentioned in the beginning of this chapter, where the individual user only establishes SLA with its first access network and the access network will negotiate a bulk SLA for its corresponding aggregate of flows with its next intermediate network. When such an aggregate exits the first network and enters the next network, the aggregate will be checked for its conformance based on the bulk SLA between these two domains. To study conformance deterioration in this scenario, the stochastic burstiness for the whole aggregate needs to be analyzed. According the superposition property of m.b.c stochastic arrival curve, an aggregate of flows with the m.b.c. stochastic arrival curves can be considered as one flow with an m.b.c. stochastic service curve. Then, the following result for an aggregate with N flows can be obtained.

Theorem 8.16 (Stochastic Burstiness for an Aggregate). *Consider an aggregate that consists of N flows with input process $A_i(t)$, $(i = 1, \ldots, N)$. Assume that, for each flow i, $A_i(t) \sim_{mb} \langle f_i, r_i \rangle$. Let $A(t) = \sum_{i=1}^{N} A_i(t)$ be the input process of the aggregate. Then, for any $t \geq 0$,*

$$A(t) \sim \left\langle g, \sum\nolimits_{i=1}^{i=N} r_i \right\rangle, \tag{8.22}$$

where

$$g(\sigma) = f_1 \otimes f_2 \otimes \cdots \otimes f_N(\sigma), \tag{8.23}$$

If all the flows in the aggregate are independent of each other,

$$g(\sigma) = 1 - \bar{f}_1 * \bar{f}_2 * \cdots * \bar{f}_N(\sigma) \tag{8.24}$$

where $\bar{f}_i(\sigma) = 1 - [f_i(\sigma)]_1$ for $i = 1, 2 \cdots N$.

Similarly, with the result above and Theorem 8.1, one can obtain a non-conformance probability bound for the aggregate of flows.

Corollary 8.17 (Non-conformance Probability Bound for an Aggregate). *Consider an aggregate that consists of N flows with input process $A_i(t)$, $(i = 1, \ldots, N)$. Assume, for each flow i, $A_i(t) \sim_{mb} \langle f_i, r_i \rangle$. The aggregate is checked for its conformance by a token bucket meter with token generation rate $\sum_{i=1}^{i=N} r_i$ and token bucket depth σ_{th}. Then, the non-conformance probability $P_{nonconf}(t)$ is bounded by*

$$P_{nonconf}(t) \leq f_1 \otimes f_2 \cdots \otimes f_N(\sigma_{th}). \tag{8.25}$$

If all the flows in the aggregate are independent of each other,

$$P_{nonconf}(t) \leq 1 - \bar{f}_1 * \bar{f}_2 \cdots * \bar{f}_N(\sigma_{th}), \tag{8.26}$$

where $f_i(\sigma) = 1 - \bar{f}_i(\sigma)$, for $i = 1, 2 \cdots N$.

8.4 Simulation Results

In this section, the analytical results are verified with simulations using ns-2 [106]. Figure 8.3 shows the network topology used in simulation, which was also used in [57], where traffic is sent from source S_i to destination D_i. There are two classes of traffic competing for resources at each node, which is a GR server implementing the WFQ scheduler. Traffic from sources S_{2i+1}, $i = 0, 1, 2$, belongs to class 1 and traffic from sources $S_{2i}, i = 1, 2$, belongs to class 2 at each node. Before entering the network, traffic from each source S_{2i+1} is shaped by a token bucket shaper to conform to a certain specification. The conformance deterioration of flow F_1 from S_1 to D_1 is investigated. The conformance of flow F_1 is checked at the output port R_3 to D_1 of node R_3 using a token bucket meter. For simplicity, Poisson sources are used for flows in traffic class 1 from S_{2i+1} to D_{2i+1}, and exponential ON/OFF sources are used for flows in traffic class 2 from S_{2i} to D_{2i} in the experiments. The theoretical results on the conformance deterioration probability for the Poisson input flow are verified. In [35], it has been shown that the queue length distribution of a Poisson traffic input with mean arrival rate λ in a constant-rate server with server rate ρ satisfies

$$\Pr(B(\infty) > x) = 1 - \left(1 - \frac{\lambda}{\rho}\right) \sum_{n=0}^{x} \frac{[\frac{\lambda}{\rho}(n-x)]^n}{n!} e^{-\frac{\lambda}{\rho}(n-x)}. \tag{8.27}$$

Clearly, by definition, Poisson traffic has a v.b.c. stochastic arrival curve whose bounding function is given by (8.27). Since the Poisson process is i.i.d., according to (3.38), Poisson traffic also has an m.b.c. stochastic arrival curve with the same bounding function given by (8.27). Therefore, the non-conformance probability bound of a Poisson traffic flow after crossing the network can be obtained by applying this bounding function to the results derived in Sections 8.2 and 8.3.

8.4.1 Per-Flow Scheduling Network in Single-Node Case

The first experiment considers the single-node case. In this case, there are only $S_1, S_2, R_1, R_2, D_1, D_2$ in the simulated network shown in Figure 8.3. Server R_1 guarantees per-flow service to flow F_1 from S_1 to D_1 since there is no other cross traffic in traffic class 1 for flow F_1. This scenario investigates the stochastic burstiness increase of flow F_1 after it passes one WFQ node R_1. Poisson source S_1 generates flow F_1 at an average rate of 45 pkts/sec. The size of each packet from flow F_1 is fixed at 128 bytes. Therefore, the average sending rate of flow F_1 is 45 kbps. For the flow F_2 from S_2 to D_2 in traffic class 2, an ON/OFF source is used that has an average sending rate of 50 kbps and packet size 5 times that of flow F_1. Only the flow F_1 is shaped by a token bucket shaper, whose token generation rate is 50 kbps and bucket depth is 15 tokens. The token size in all experiments is 128 bytes. The access

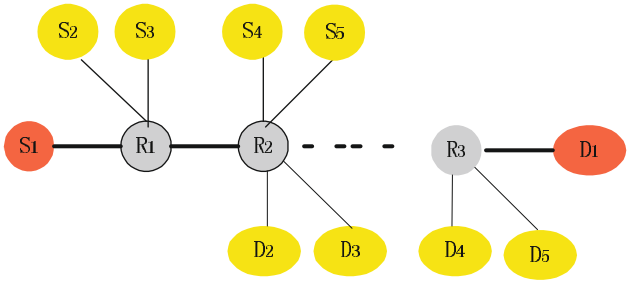

Fig. 8.3. Network topology used in simulation

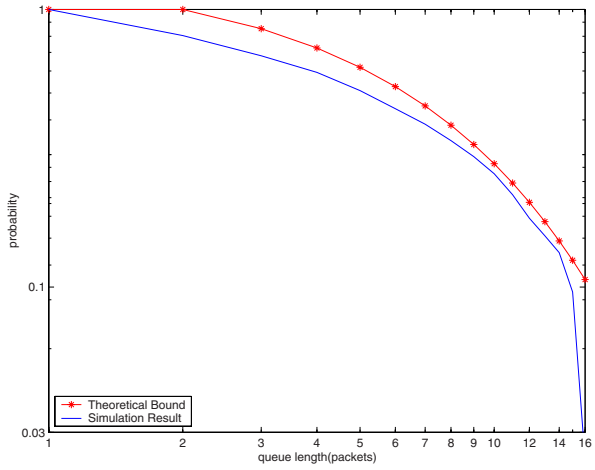

Fig. 8.4. Queue length tail distribution after crossing a single node in a per-flow scheduling network

link capacity of link S_1 to R_1 is 10 Mbps. The network core link capacity of R_1 to R_2 is 200 kbps and the weight ratio between class 1 and class 2 is 1 : 1 for the WFQ node in the core network. Flow F_1 belongs to class 1 and F_2 belongs to class 2. The link capacity of the last hop is 50 kbps. The last hop R_2 to D_1 for F_1 is a constant-rate server, since there is no other traffic sharing this link, that has the same rate as the token generation rate of the token bucket shaper. The queuing length distribution at this hop is the virtual queuing length distribution for flow F_1, which is used to measure the stochastic burstiness of the output traffic.

Figure 8.4 shows the simulated queue length tail distribution of flow F_1 at the last hop, where the theoretical bound is obtained by substituting x with $x - \rho\left(T + \frac{L_{\max,1}}{R}\right)$ in (8.27) according to Corollary 8.4. For a WFQ scheduler

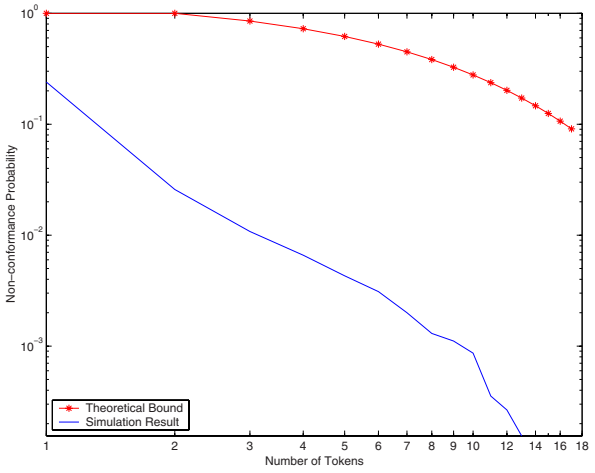

Fig. 8.5. Non-conformance probability after crossing a single node in a per-flow scheduling network

here, $T = \frac{L\max}{C}$, where C is its total capacity and $L_{\max}$ is the maximum packet size among all flows in the same server. $L_{\max,1}$ is the maximum packet size for F_1 and R is the reserved rate for F_1. The unit for the queue length is a packet that has the same size as the packets from flow F_1. As can be seen from the figure, although flow F_1 becomes more bursty after passing through node R_1 since its virtual queue length exceeds the token bucket depth 15, its burstiness increase remains bounded by the theoretical result.

Next, the result for the non-conformance probability bound is verified. Figure 8.5 shows the simulated non-conformance probability and its theoretical bound. For this, a token bucket meter with the same token generation rate (50 kbps) as the token bucket shaper is placed at the last hop of flow F_1 to check its conformance. The same experiment settings described above were adopted, except that the bucket depth of the token bucket shaper at the ingress and the token bucket meter at the last hop were changed in order to investigate the effect on the non-conformance probability of flow F_1. Note that the token bucket shaper at the ingress node and the token bucket meter at the last hop have the same parameters in all experiments in order to check conformance for the considered flow F_1. To obtain the non-conformance probability bound, the following procedures are used:

1. Determine the initial bounding function for the input flow F_1 with rate $r = 50$ kbps by using Equation (8.27).

2. Determine the bounding functions for the stochastic burstiness of the flow under consideration after passing through a token bucket shaper according to Theorem 8.2.

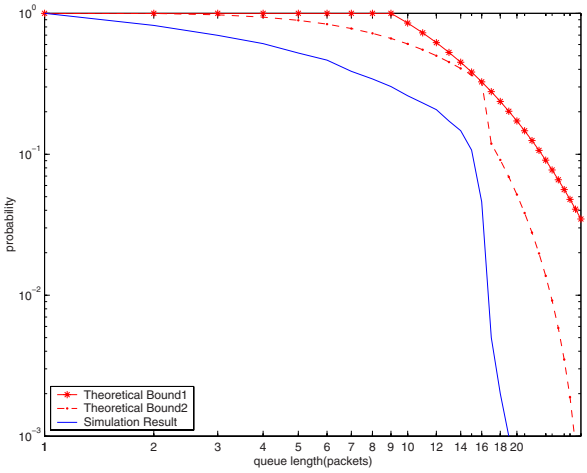

Fig. 8.6. Queue length tail distribution after crossing a single node in an aggregate scheduling network

3. Obtain the non-conformance probability bound for different token bucket depths σ_{th} by using the inequality (8.4) in Corollary 8.4.

Figure 8.5 shows the simulated non-conformance probability and its theoretical bound.

8.4.2 Aggregate Scheduling Network in Single-Node Case

The second experiment considers the single node case in an aggregate scheduling network. In this experiment, all other settings are exactly the same as in the first experiment except that a cross flow F_3 from S_3 to D_3 with the same source setting (including token bucket shaping) as flow F_1 enters the network and competes for resources with flows F_1 and F_2 at the WFQ node R_1. F_1 and F_3 are aggregated in the same class (class 1) to verify the analytical results on the aggregate scheduling network. Flow F_2 belongs to class 2.

Figure 8.6 shows the simulated queue length distribution of flow F_1 at its last hop. The theoretical bound 2 is obtained by Theorem 8.11, in which the stochastic service curve is derived from Lemma 8.10. The theoretical bound 1 in Figure 8.6 is derived from Theorem 8.6. Figure 8.6 shows that the theoretical bound 2 is tighter than the theoretical bound 1. This results from the fact that Theorem 8.11 makes use of the stochastic service curve offered to flow F_1 by the WFQ node under aggregate scheduling, which can be derived from Lemma 8.10. In contrast, Theorem 8.6 uses the worst-case service curve offered to the flow by the node under aggregate scheduling, which was derived based on results from Theorem 2.27.

Next, the result for the non-conformance probability bound is verified with the same experiment settings described above except that the bucket depth of

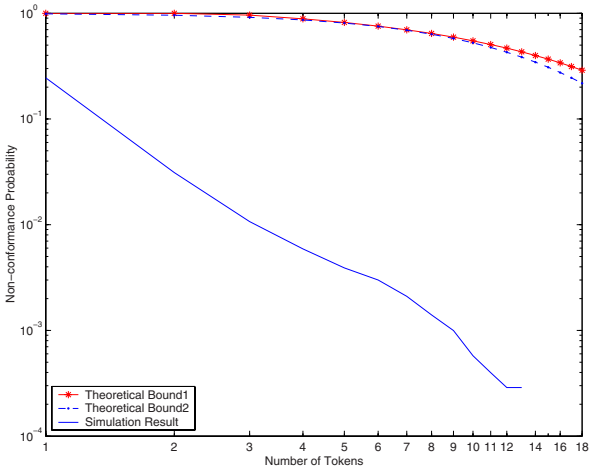

Fig. 8.7. Non-conformance probability after crossing a single node in an aggregate scheduling network

the token bucket shaper at the ingress node and the token bucket meter at the last hop are changed in order to investigate the effect on the non-conformance probability of flow F_1. For the same reason as mentioned above, Figure 8.7 shows that the theoretical non-conformance probability bound 2 is also tighter than the theoretical non-conformance probability bound 1.

8.4.3 Aggregate Scheduling Network in Multi-node Case

In the third experiment, the simulated network topology is exactly the same as that shown in Figure 8.3. Traffic from sources S_{2i+1}, $i = 0, 1, 2$, belongs to class 1 and traffic from sources $S_{2i}, i = 1, 2$, belongs to class 2 in each node. All other settings are the same as in the experiments discussed above except that Poisson sources S_{2i+1} generate flow F_{2i+1} at an average rate of 45 pkts/sec and exponential ON/OFF flows F_{2i} from S_{2i} to D_{2i} have an average sending rate of 50 kbps and packet size five times that of flow F_{2i+1}. The stochastic burstiness increase of flow F_1 is explored to verify the analytical results on aggregate scheduling in the multi-node case.

Figure 8.8 shows that after passing through two WFQ nodes, flow 1 becomes more bursty since the simulated result shows that, at its last hop, the queue length, which implies burstiness, can be larger than 15, the depth of the token bucket shaper. Nevertheless, the simulation results are bounded by the theoretical bound 1 derived from Theorem 8.6 and theoretical bound 2 derived from Theorem 8.11 by applying (8.27) to these two theorems. For the same reason as explained in the second experiment above, theoretical bound 2 is shown to be tighter than theoretical bound 1, as expected.

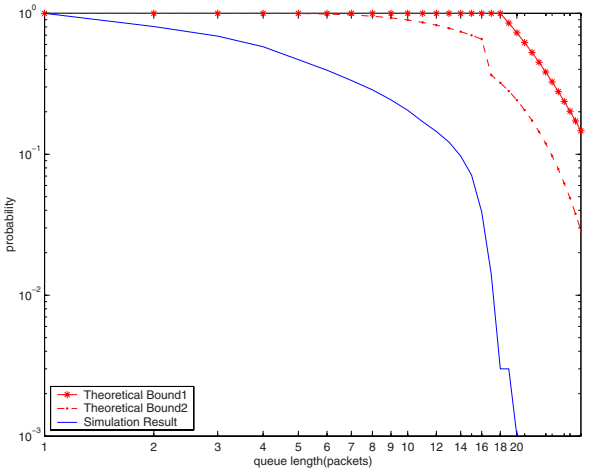

Fig. 8.8. Queue length tail distribution after crossing multi-nodes in an aggregate scheduling network

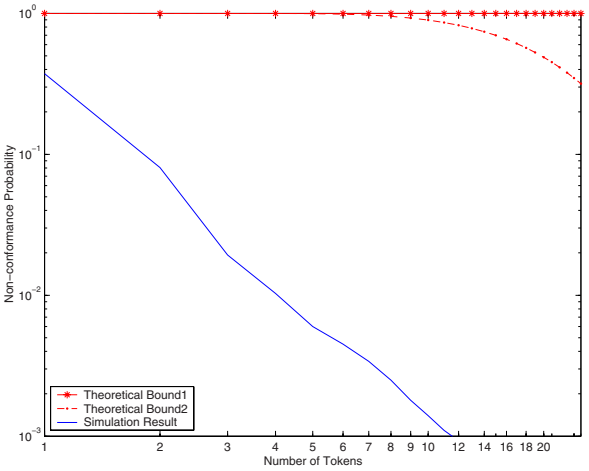

Fig. 8.9. Non-conformance probability after crossing multi-nodes in an aggregate scheduling network

The result on the non-conformance probability bound is also verified with the same experiment settings, except that the bucket depth of the token bucket shaper at the ingress node and the token bucket meter at the last hop are changed in order to investigate the effect on the non-conformance probability of flow F_1. To obtain the non-conformance probability bound, the following procedures are used:

1. Determine the initial bounding functions for the stochastic burstiness of F_1 with rate 50 kbps and each cross-flow with rate $r^{h_i} = 50$ kbps according to (8.27).

2. Determine the bounding functions for the stochastic burstiness of F_1 after passing through a token bucket shaper according to Theorem 8.2.

3. Convert each aggregate scheduling server (providing a service curve to the aggregate) to a per-flow scheduling server (providing a stochastic service curve to the flow) according to Lemma 8.10.

4. Obtain the end-to-end non-conformance probability bound for different token bucket depths σ_{th} by using the inequality (8.21) in Theorem 8.15.

Figure 8.9 shows the non-conformance probability of flow F_1 after passing through two WFQ nodes and the corresponding theoretical bounds. It is shown that the theoretical bound 1 derived from Theorem 8.6 is close to 1, which is overly conservative. The reason is that Theorem 8.6 uses the worst-case deterministic per-flow service curve and each server will make the original burstiness bounding function of flow F_1 shift to the right by some constant amount according to Theorem 8.6 and then the bound will be 1 in the range between 0 and the accumulation of the constant amount. Therefore, if the accumulation of the constant amount due to shifting is greater than the token bucket depth, the non-conformance deterioration probability bound derived from Theorem 8.6 will be close to 1, which is overly conservative and indeed useless as a bound. On the other hand, since the theoretical bound 2 derived from Theorem 8.11 makes use of the stochastic service curve instead of the worse case deterministic service curve, the bound is tighter than the theoretical bound 1.

8.5 Summary and Bibliographic Comments

In this chapter, we have analytically studied the conformance deterioration problem in networks with service level agreements. We first established the relationship between conformance deterioration and the stochastic burstiness increase of a flow. Then, based on the analysis in previous chapters, the stochastic characterization of the flow was utilized to analyze the stochastic burstiness increase in a per-flow scheduling network and an aggregate scheduling network.

To investigate the stochastic per-flow burstiness increase for individual flows in the aggregate scheduling network, we also investigated the stochastic behavior of a server providing deterministic service to the aggregate of flows.

As discussed in Chapters 5 and 6, an aggregate scheduling server providing a service curve to an aggregate can be regarded as a per-flow scheduling server providing a stochastic service curve to each individual flow in the aggregate. This has helped improve the bound on conformance deterioration. Furthermore, we have applied the concatenation property for analysis of stochastic burstiness increase. These results are not only useful for the analysis of the situation presented in this chapter but also shed some light on conformance analysis in aggregate scheduling networks with other general topologies.

As shown by the simulation results in Section 8.4, there is still some room for improvement on the non-conformance probability bound. The non-conformance probability bound may be improved by further research. Note that Figures 8.4, 8.6, and 8.8 show that the theoretical bounds on the queue length tail distribution of output flows in the virtual queuing system are close to the simulation results. However, the non-conformance probability checked by the token bucket meter is bounded by the probability that the queue length of the output flow in the virtual queuing system exceeds the token bucket depth, as shown in Theorem 8.1. Therefore, the major cause for the looseness of the non-conformance bounds is the difference between the non-conformance probability and the probability that the queue length in the virtual queuing system exceeds a certain threshold. Further study on the differences between the token bucket meter and the virtual queuing system may lead to a much tighter non-conformance probability bound.

The content of this chapter is mainly based on [99] by Liu, Tham and Jiang. The problem of conformance deterioration was initially investigated by Guerin and Pla [57] through extensive simulations. They studied the conformance deterioration caused by interactions among flows aggregated in the same traffic class. Both per-flow and per-aggregate conformance deterioration were investigated in [57]. The authors observed through simulations the impact of link load, number of cross flows and number of hops traversed by the flow on conformance deterioration. However, [57] does not provide any analytical study on what is the extent to which a flow becomes non-conformant after crossing a network.

Besides [57], there are several other works addressing related issues that use different methods. The work in [56] investigated the distortion of a constant bit rate (CBR) flow when it is aggregated with other flows after crossing several network elements. The work in [120] extended the results in [56] to consider the same issue with variable packet sizes. Another related work is [97], which studied conformance deterioration in a single-node case, a radio access network under the UMTS framework.

Problems

8.1. Prove Theorem 8.6.

8.2. Consider a system with the same setting as the example shown in Section 8.4.1 except that each flow has the same *m.b.c.* stochastic arrival curve, $\langle e^{-0.25t}, 50\text{kbps} \rangle$. Find the non-conformance probability for F_1.

8.3. Consider a system with the same setting as the example shown in Section 8.4.2 except that each flow has the same *m.b.c.* stochastic arrival curve, $\langle e^{-0.25t}, 50\text{kbps} \rangle$. Find the non-conformance probability for F_1.

8.4. Consider a system with the same setting as the example shown in Section 8.4.3 except that each flow has the same *m.b.c.* stochastic arrival curve, $\langle e^{-0.25t}, 50\text{kbps} \rangle$. Find the non-conformance probability for F_1.

8.5. For the system shown in Problem 8.2, if there is an impairment process I for the server, assume $I \sim_{mb} \langle e^{-0.25t}, 50\text{kbps} \rangle$. Find the non-conformance probability for F_1.

8.6. For the system shown in Problem 8.3, if there is an impairment process I for the server, assume $I \sim_{mb} \langle e^{-0.25t}, 50\text{kbps} \rangle$. Find the non-conformance probability for F_1.

8.7. For the system shown in Problem 8.4, if there is an impairment process I for each server, assume $I \sim_{mb} \langle e^{-0.25t}, 50\text{kbps} \rangle$. Find the non-conformance probability for F_1.

8.8. Under the same condition as in Theorem 8.12 except that β is a strict service curve and there is an impairment process $I \sim_{mb} \langle f_i, \alpha_i \rangle$ for the server, find the non-conformance probability for flow f.

8.9. Under the same condition as in Theorem 8.13 except that β is a strict service curve and there is an independent impairment process $I \sim_{mb} \langle f_i, \alpha_i \rangle$ for the server, find the non-conformance probability for flow f.